

THE GROWTH & MIGRATION OF JOVIAN PLANETS IN EVOLVING PROTOSTELLAR DISKS WITH DEAD ZONES

SOKO MATSUMURA¹

Department of Physics & Astronomy, Northwestern University, Evanston, IL, 60208 USA

RALPH E. PUDRITZ

Department of Physics & Astronomy, McMaster University, Hamilton, ON, L8S 4L8 Canada

AND

EDWARD W. THOMMES

Department of Physics, University of Guelph, Guelph, ON, N1G 2W1 Canada

Draft version November 23, 2018

ABSTRACT

The growth of Jovian mass planets during migration in their protoplanetary disks is one of the most important problems that needs to be solved in light of observations of the small orbital radii of exosolar planets. Studies of the migration of planets in standard gas disk models routinely show that the migration speeds are too high to form Jovian planets, and that such migrating planetary cores generally plunge into their central stars in less than a million years. In previous work, we have shown that a poorly ionized, less viscous region in a protoplanetary disk called a *dead zone* slows down the migration of fixed-mass planets. In this paper, we extend our numerical calculations to include dead zone evolution along with the disk, as well as planet formation via accretion of rocky and gaseous materials. Using our symplectic-integrator-gas dynamics code, we find that dead zones, even in evolving disks wherein planets grow by accretion as they migrate, still play a fundamental role in saving planetary systems. We demonstrate that Jovian planets form within 2.5 Myr for disks that are ten times more massive than a minimum mass solar nebula with an opacity reduction and without slowing down migration artificially. Our simulations indicate that protoplanetary disks with an initial mass comparable to the minimum mass solar nebula (MMSN) only produce Neptunian mass planets. We also find that planet migration does not help core accretion as much in the oligarchic planetesimal accretion scenario as it was expected in the runaway planetesimal accretion scenario. Therefore we expect that an opacity reduction (or some other mechanisms) is needed to solve the formation timescale problem even for migrating protoplanets, as long as we consider the oligarchic growth. We also point out a possible role of a dead zone in explaining long-lived, strongly accreting gas disks.

Subject headings: accretion, accretion disks - turbulence - planetary systems: formation - planetary systems: protoplanetary disks - planets and satellites: general - Solar system: formation - stars: pre-main-sequence

1. INTRODUCTION

The properties of nearly 300 recently discovered extra-solar planetary systems reveal that Jovian mass planets are often found at a scaled orbital radius of Mercury around their central stars (e.g. Udry & Santos 2007). Since none of the current theories of Jovian planet formation can explain *in situ* formation of gas giants at these small distances from their stars, it is generally agreed that such planets were formed in the outer regions of protoplanetary disks and migrated through them to their current positions (Lin et al. 1996). Growth of giant planets takes place during this passage and both processes are terminated when most of the gas in the protoplanetary disk is either accreted onto the central star, or dissipated by photoevaporation (e.g. Shu et al. 1993; Hollenbach et al. 1994; Alexander et al. 2006). Observations of infrared to submm emission and gas accretion rates onto the central stars reveal that disk lifetimes are typically 1 – 10 Myr (e.g. Hartmann et al.

1998; Muzerolle et al. 2000; Andrews & Williams 2005; Sicilia-Aguilar et al. 2006).

The observed disk life-times raise two difficulties in planet formation theory. The first regards planet migration: the migration time scales of planets arising from the tidal interaction between a planet and the gas disk are shorter than the disk lifetimes. Therefore, unless they are stopped by some robust mechanism, planets plunge into their central stars within about a million years. The second is specific to core-accretion model for Jovian planet formation: the formation time scales may be longer than, or comparable to, the disk life times. Therefore, unless the formation time scale is reduced somehow, the existence of giant planets cannot be explained by the core accretion scenario.

The core-accretion model posits that gas giants result from a two-stage process - the first being the formation of their rocky cores by the repetitive coagulation and agglomeration of the smaller bodies onto the larger ones (as in the terrestrial planet formation), and the second being the accretion of their massive gaseous envelope from the

¹ This work was done while at McMaster University.

surrounding disk.

In the first stage, the formation of the rocky core proceeds as bodies grow from a micron to a planetary size. One of the difficulties occurs when particles grow up to dm sizes. At this point, the collisional agglomeration may not be a preferred path to make the larger bodies (Langkowski et al. 2008). Even if the sticking is still efficient and the bodies can keep on growing, the gas drag becomes non-negligible for such objects. Since the gas disk rotates at the sub-Keplerian speed, slightly slower than these growing bodies, the bodies feel the head wind, lose the angular momentum, and eventually migrate into the central star. Migration induced by gas drag becomes most efficient for meter-sized bodies, and becomes negligible again for the km-sized bodies since they are large enough not to be affected by the gas drag (Weidenschilling 1977). The gravitational instability in the planetesimal disk was suggested to avoid this meter-size barrier (Goldreich & Ward 1973). However, such a mechanism may be hindered by the Kelvin-Helmholtz instability (Cuzzi et al. 1993; Weidenschilling 1995) unless the local solid-to-gas ratio is sufficiently high (e.g. Sekiya 1998; Youdin & Shu 2002). Recently, it was demonstrated that very rapid planetesimal growth up to Ceres-mass objects is possible via a streaming instability in such turbulent disks (e.g. Johansen & Youdin 2007; Youdin & Johansen 2007). Therefore, there is good justification to skip these early stages, and to assume that there are already km-sized planetesimals as well as planetary embryo(s) which are embedded in a gas disk. In this paper, we will follow this approach as the previous studies did.

In the second stage, protoplanetary cores keep on accreting planetesimals while they start developing gaseous envelopes. A cornerstone work done by Pollack et al. (1996) (P96 hereafter) identified three phases in giant planet formation. The first phase is a rapid core building phase, in which a protoplanetary core of $0.6M_E$ grows up to $\sim 10M_E$ within half a million years. The second phase is a slow gas and planetesimal accretion phase which lasts until the crossover mass (for which the envelope mass is comparable to the core mass) is reached. The third phase is a rapid gas and planetesimal accretion phase, in which the planet quickly becomes a gas giant. P96 showed that planet formation spends most time in the second phase that could last for several million years. Since this is uncomfortably close to a typical disk life time, it was considered as one of the weakest points of core accretion scenario (e.g. Boss 1997). To shorten the second phase, protoplanets could either increase the gas accretion rate itself, or increase the planetesimal accretion rate and expand the gas feeding zone. Ikoma et al. (2000); Hubickyj et al. (2005) (hereafter INE00, and HBL05 respectively) took the former approach, and considered a reduced opacity in planetary envelopes. HBL05 used an updated version of the code by P96 with a more recent opacity table, and showed that smaller opacity, which mimics the dust settling and coagulation in the protoplanet’s atmosphere, decreases the effective gas pressure of the protoplanetary envelope, and hence leads to the faster gas accretion. They showed that the *in situ* formation timescale of Jupiter could be as short as 1 Myr if the opacity is 2% of the interstellar value and the core mass is $10M_E$. On the other hand, Alibert et al. (2005)

(hereafter A05) took the latter approach, and considered planet formation during migration. In P96, planetesimal accretion slows when the planetesimals get depleted in the feeding zone, because a planet has to accrete gas and expand its feeding zone to further accrete planetesimals. Since the gas accretion in Phase 2 tends to be slower than the planetesimal accretion in Phase 1, it takes longer to accrete a similar amount of gas envelope to the core, and achieve a crossover mass. A05 overcame this problem by including disk evolution and planet migration in the model, so that the planetesimal feeding zone is constantly replenished. The gas accretion time shortens as the planetary mass increases, because it proceeds on the Kelvin-Helmholtz timescale, which is a steep function of planetary mass. They showed that the Jupiter formation timescale could be of the order of 1 Myr if the planet migrates. However, as noted by Ward (1997), solving the accretion problem by migration in a standard disk model is a “double-edged sword”, since it comes at the price of possibly losing the planets to their central star. Thus, A05 assumed that some unspecified mechanism would slow down the fast type I (pre-gap opening) migration by factors of 10 – 100 times compared to the migration estimated in a 3D disk by Tanaka et al. (2002).

Here, we propose a possible mechanism which can slow planet migration, and investigate planet formation in that context. In a standard disk with a smooth surface mass density and a standard viscosity expected from the MRI turbulence, both type I and II migration time scales are shorter than the disks’ life times. The most popular source of such a viscosity is the magneto-rotational instability (MRI, Balbus & Hawley 1991). However, it has been demonstrated by several groups that protoplanetary disks are not MRI active everywhere, but harbor extended regions known as the dead zones (Gammie 1996) where there is virtually no turbulence². Many authors have studied the physical extent of the dead zones by using different disk models and taking account of a variety of the ionization/recombination processes (e.g. Glassgold et al. 1997; Sano et al. 2000; Fromang et al. 2002; Semenov et al. 2004; Matsumura & Pudritz 2003, 2006, hereafter MP03, and MP06 respectively). These models suggest roughly the same size of the dead zones (from < 1 AU to 10–20 AU), indicating that a dead zone is a robust feature of a protoplanetary disk. Since this is a critical region of a disk both for planet formation and migration, it is of vital importance to investigate these problems in the context of protoplanetary disks with dead zones. Recent numerical simulations of such a layered disk have shown that the expected viscosity parameter α is about 10^{-2} in the active zone and 10^{-4} – 10^{-5} in

² This arises in principal because operation of the MRI requires good coupling between the gaseous disk and the magnetic field. However, the ionization fraction in the inner regions of dense protoplanetary disks is typically so low that Ohmic diffusion prevents the growth of the MRI in such regions. The size of the dead zone can be computed once the source of disk ionization (e.g. stellar X-rays, cosmic rays) is known. Assuming that the MRI is the dominant source of the disk’s “turbulent” viscosity, the dead zone is nearly inviscid. The existence of a dead zone in a protoplanetary disk was first proposed by Gammie (1996) who showed that there is a magnetically dead zone in the inner disk where cosmic rays cannot penetrate (assuming the cosmic ray stopping density is 98 g cm^{-2}), and that such a region is sandwiched by the magnetically active surface layers where gas accretes toward the star efficiently.

the dead zone (Fleming & Stone 2003). Therefore, if the MRI is the dominant source of the disk viscosity, a significant decrease in viscosity is expected within the dead zone, which most likely affects the rate of planet migration. Moreover, recent observations have revealed that disk's viscosity parameters may take a larger range than previously expected; $\alpha = 10^{-6} - 10^{-1}$ (Hueso & Guillot 2005; Luhman et al. 2007), indicating that at least some observed disks may possess a low viscosity region like a dead zone.

In an earlier paper, we have demonstrated that dead zones can significantly slow the rate of migration of planets, and save planetary systems from plunging into the central stars (Matsumura et al. 2007, hereafter MPT07). In particular, we found (1) type II migration (post-gap-opening migration) is slowed in the dead zone due to the low viscosity there, (2) even low-mass planets ($\leq 10M_E$), which are usually type I migrators (i.e. non gap-openers), may open a gap in the dead zone if the thermal condition is satisfied, and thus migrate slower there, and (3) type I migrators moving toward the dead zone can be stopped at the outer edge of the dead zone due to the jump in mass density there which is a result of the slower advection speed inside the dead zone with respect to outside it.

In this paper, we present a rather complete treatment of the formation and migration of Jovian planets within their evolving protoplanetary disks. We compute comprehensive time-dependent models for the growth of Jovian planets in the core accretion picture in viscously evolving gaseous disks. Our calculations include updates on both stages of accretion (planetesimals and gas), as well as the ability to follow planetary migration down to 0.1 AU. We approach this problem by means of time-dependent simulations that track both planetary accretion and migration through disks with evolving dead zones. There are two major effects of disk evolution in our models: (i) the gradual accretion of mass from the disk onto the star which limits the reservoir that is available to the growing Jovian planet; and (ii) the shrinkage of the size of the dead zone as a consequence of mass accretion onto the star (mainly) through the well coupled surface layers of the disk. This process reduces the size of the dead zone substantially with time — perhaps leaving it only a few AU in extent after a million years.

We first introduce our disk models and numerical methods in §2. We also highlight a possible role of dead zones in disk accretion onto the central stars. Then we study planet formation in an inviscid disk, and compare our results with P96, and HBL05 (§3). We also check the effect of the opacity, and compare the results with HBL05, which improved the work of P96 and further investigated the opacity effects. We then go on to compute planet formation and migration in an evolving disk, and compare the results with A05 in §4. The culmination of our work is presented in §5 where we generalize our results and present planet formation in an evolving disk with a dead zone. Finally, we summarize our work in §6.

2. NUMERICAL METHODS AND DISK MODELS

In this section, we introduce the numerical code that we use to simulate planet formation in a realistic protoplanetary disk. We focus on the newly added features and refer the reader to our previous paper (MPT07) for

details of the basic code. We also summarize the initial conditions chosen for the runs in the following sections.

We perform numerical simulations of planet formation and migration by using a hybrid numerical code, which combines an N-body integrator with a simple disk evolution code (Thommes 2005). The N-body part is based on the symplectic integrator called SyMBA (Duncan et al. 1998), which has improved the N-body map of Wisdom & Holman (1991) with an adaptive timestep to handle the close encounters among massive bodies. The gaseous disk part of the code evolves a disk viscously as well as through angular momentum exchange with the embedded planets according to a general Navier-Stokes equation. By following the standard prescription by Lin & Papaloizou (1986), the gas disk is divided into radial bins, which represent annuli of disks with azimuthally and vertically averaged properties like surface mass density, temperature, and viscosity. Viscous evolution of the disk is calculated by specifying the standard alpha viscosity (Shakura & Sunyaev 1973) for each bin, while the effect of disk-planet interactions is added in the form of the torque density as in Ward (1997); Menou & Goodman (2004).

The code is also modified to simulate planet formation, which consists of planetesimal and gas accretion. For planetesimal accretion, as it was mentioned in §2, the transition between runaway, and oligarchic phases occurs once the protoplanet becomes locally large enough to perturb the surrounding smaller planetesimals and increase their random velocities, which decreases the collisional crosssection, and therefore leads to the longer accretion time (Ida & Makino 1993; Kokubo & Ida 1998). This critical mass is about a few times 10^{-3} Moon masses or less (Thommes et al. 2003). Since all of our simulations start with $0.6 M_E$, we can safely assume that the oligarchic growth is the dominant planetesimal accretion phase in our case.

The planetesimal accretion part of the code was developed by Thommes et al. (2003) to handle the *oligarchic* growth, which is the slower planetesimal accretion phase following the rapid planetesimal accretion (Ida & Makino 1993; Kokubo & Ida 1998). Here, we follow the previous studies (e.g. Kokubo & Ida 1996; Thommes et al. 2003), and assume (1) dynamical friction by smaller planetesimals on larger ones is effective, so that larger planetesimals have smaller velocities than smaller ones, and (2) gravitational focusing is effective, so that the relative velocities between two colliding bodies are smaller than the escape velocities from the larger ones, and therefore collisions effectively lead to coagulation. Accretion rate of planetesimals with mass m onto a protoplanet with mass M_p is written as

$$\frac{dM_p}{dt} \sim \frac{C \Sigma_{solid} M_p^{4/3}}{e_m^2 a^{1/2}}, \quad (1)$$

where $C = 6\pi^{2/3}[3/(4\rho_M)]^{1/3}(G/M_*)^{1/2}$, ρ_M is the bulk density of a protoplanet, Σ_{solid} is the surface mass density of a planetesimal disk, and e_m is the eccentricity of planetesimals. We assume that the protoplanet accretes planetesimals within its feeding zone of $10R_{Hill}$ ($R_{Hill} = (M_p/(3M_*))^{1/3}a$ is the Hill radius of the protoplanet), which is a typical orbital separation between protoplanets (Kokubo & Ida 1998).

The gas accretion part of the code estimates the planetary mass increase by calculating the gas accretion timescale and radius (see §2.1 for details). Instead of solving the planetary structure equations directly to estimate the gas accretion rate as in P96, HBL05, and A05, we calculate the gas accretion timescale based on these previous studies, and let the protoplanetary core accrete gas inside the accretion radius on the estimated timescale.

We also add a new capability to our disk model to include the evolution of a dead zone due to the faster accretion through the well coupled surface layers onto the central star. This is further explained in §2.2.

2.1. Gas accretion prescription

Since the planetesimal accretion prescription is discussed in detail elsewhere (Thommes et al. 2003), we focus on the gas accretion prescription added to the code in this subsection. Gas accretion onto a protoplanet has been studied either by solving the planetary structure equations (e.g. P96, HBL05, INE00, and A05), or by performing the hydrodynamic (HD) simulations (e.g. Bryden et al. 1999; Lubow et al. 1999; Kley et al. 2001; D’Angelo et al. 2002; Tanigawa & Watanabe 2002; D’Angelo et al. 2003; Bate et al. 2003). The main focus of the former studies is on the core-building phase to the rapid gas accretion phase, while that of the latter ones is on the final stage of gas accretion where a massive planet accretes from its subdisk. Since the former studies except A05 treat the gas disks rather simply by assuming that the protoplanetary feeding zone is always replenished, they have a relatively crude estimate of the available amount of gas in the feeding zone. Therefore, they tend to overestimate the gas accretion for a planet which is massive enough to open a gap. The gas accretion in the latter case is regulated by the subdisk formed around the planet. Since these studies do not include the contraction of the protoplanetary atmosphere, they tend to overestimate how quickly a protoplanetary core can actually accrete gas. Here, we try to combine the strengths of these two methods, and use three different gas accretion rates depending on presence/absence of planetesimal accretion, and circumplanetary disk accretion.

The presence, or absence of planetesimal accretion affects the efficiency of gas accretion. INE00 suggested that, when the planetesimals are accreting concurrently with the gas, the thermal energy released in the bombardment of planetesimals provides extra pressure support for the gaseous envelope of the protoplanet, and therefore the gas accretion slows down. They found that such an accretion rate could differ from the accretion rate without planetesimal accretion by several times, which are plotted in Fig. 1 as two parallel lines. They also studied the effects of core mass and dust opacity on gas accretion, and showed that there is an optimal core mass which results in efficient gas accretion. If planetesimal accretion is cut off long after the protoplanet starts accreting gas actively, the gas accretion time becomes longer. This is because the radiative loss is mostly compensated by planetesimal accretion rather than gas accretion (i.e. gravitational energy release due to the envelope contraction). On the other hand, if planetesimal accretion is cut off while the core is still small, the gas accretion time is also prolonged, because the smaller mass

leads to the smaller radiative loss and hence the slower envelope contraction.

The final stage of gas accretion is likely to be controlled by the subdisk around a planet (Tanigawa & Watanabe 2002; Bate et al. 2003; D’Angelo et al. 2003). Gas accretion through subdisks becomes less efficient for more massive planets because the planets open a wider and deeper gap (e.g. Bate et al. 2003). The effect is seen in the parabola-like curve in Fig. 1 by D’Angelo et al. (2003). This, however, is not clear in (Tanigawa & Watanabe 2002, hereafter TW02)’s case (the lower dotted line), because they don’t take account of a gap-opening effect. In other words, their gas accretion rate is the “raw” accretion rate of the planet. Below the critical mass for subdisk accretion, gas accretion is expected to be controlled by the contraction of protoplanetary atmosphere. Therefore, we apply the KH timescale for small protoplanets, and subdisk accretion timescale for larger protoplanets.

Following these studies, we define three stages of the gas accretion; (1) gas accretion while planetesimal accretion is on-going, (2) gas accretion after planetesimal accretion ceases, and (3) gas accretion through the subdisk around the planet. Fig. 1 presents a compilation of these gas accretion timescales obtained from different studies. Two parallel descending lines are gas accretion time scales while planetesimal accretion is on-going (upper line) and after it ceases (lower line) respectively (INE00, see Eq. (1) and (2)). For comparison, accretion time scales obtained from P96 is shown in the upper dotted line. These descending trends predict shorter accretion timescales for larger planets because the models don’t take account of disk evolution effects nor planetary subdisks. On the other hand, the parabola-like relation is based on the HD simulation by D’Angelo et al. (2003), which predicts much longer gas accretion timescale for larger planets due to gap opening and accretion via circumplanetary disks. A similar study done by TW02 without a gap-opening effect is shown in the lower dotted line. Possible gas accretion timescales throughout planet formation are shown in solid curves.

(1) When there is planetesimal accretion as well as gas accretion, we follow the timescale by INE00 (the upper line of the solid parallel lines):

$$\tau_1 = 6. \times 10^8 \left(\frac{M_p}{M_*} \right)^{-2.5} \left(\frac{\kappa}{1 \text{ cm}^2 \text{ g}^{-1}} \right), \quad (2)$$

where κ is the dust opacity in the planetary envelope.

(2) When the planetesimal accretion ceases, but the gas accretion is still on-going, we adopt the timescale by INE00 (the lower line of the solid parallel lines):

$$\tau_2 = 1. \times 10^8 \left(\frac{M_p}{M_*} \right)^{-2.5} \left(\frac{\kappa}{1 \text{ cm}^2 \text{ g}^{-1}} \right). \quad (3)$$

Both of the above equations show shorter accretion timescales as the planetary mass grows.

(3) When a protoplanet becomes large enough to have a subdisk, the gas accretion timescale can be described by D’Angelo et al. (2003):

$$\tau_3 = \frac{M_p}{M_p} \quad (4)$$

$$\log \left(\frac{\dot{M}_p}{M_E \text{ yr}^{-1}} \right) = \left(18.47 + 9.25 \log \left(\frac{M_p}{M_*} \right) + 1.266 \log \left(\frac{M_p}{M_*} \right)^2 \right) \quad (5)$$

The transition of the first to the second phase occurs when the core accretion rate drops to zero. The transition of the second to the third phase occurs when $\tau_2 \sim \tau_3$. For a standard opacity $\kappa \sim 1 \text{ cm}^2 \text{ g}^{-1}$, the crossover mass is about $70 M_E$ as it can be seen in Fig. 1.

A protoplanet accretes gas within its accretion radius on each of these time scales. As in P96, the accretion radius for Eq. 2 and 3 is set to either Hill ($R_{\text{Hill}} = (M_p/(3M_*))^{1/3}a$), or Bondi ($R_{\text{Bondi}} = GM_*/c_s^2$, where c_s is sound speed) radius, whichever is smaller. On the other hand, the accretion radius for Eq. 5 is chosen to be $2R_{\text{Hill}}$, which is motivated by numerical studies like D’Angelo et al. (2003).

2.2. Accretion histories in disks with dead zones

Although our disk model is one-dimensional, it is still possible to include the effects of azimuthal and vertical structure through disk parameters in an averaged way. The difference in disk evolution due to a vertical structure becomes particularly important for a disk with a dead zone. Generally, a dead zone is sandwiched between the upper and lower turbulent surface layers where the disk is well-ionized (Gammie 1996) and hence the MRI is active. Therefore, the mass accretion is expected to be more efficient in active layers than in the dead zone. In MPT07, we did not include this effect, and hence found very little decrease in disk mass even after 10^7 years.

Here, we take account of the effects of disk’s vertical structure in the following simple way. The mass accretion through the active layers and the dead zone toward the central star can be written as the summation of accretion rates in the active layers and the dead

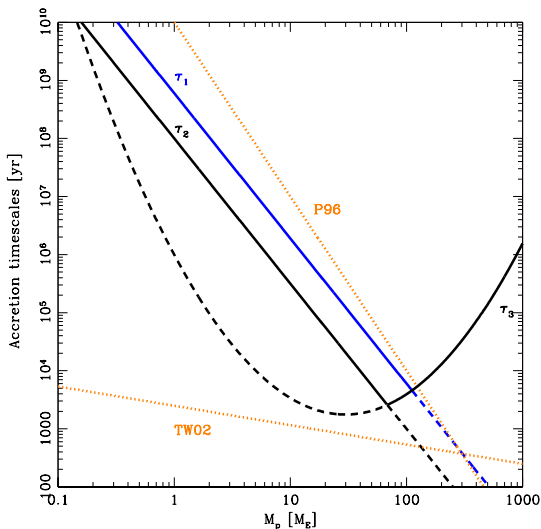


FIG. 1.— Comparison of gas accretion timescales as a function of planetary mass. The descending solid and the upper dotted line are the gas accretion timescales for the envelope contraction phase, while a parabola and the lower dotted line are those for the subdisk accretion phase. The upper dotted line is the gas accretion rate estimated from the simulation of P96. Blue line (the upper of the parallel lines) is gas accretion while planetesimal accretion is on-going, while black one (the lower of the parallel line) is that after planetesimal accretion ceases. Both of them are based on the study by INE00. Black parabola and the lower dotted line are the subdisk accretion timescales from D’Angelo et al. (2003) and TW02, respectively. The subdisk accretion by D’Angelo et al. (2003) appears to be slower than TW02 since the gap-opening effect of a planet is included.

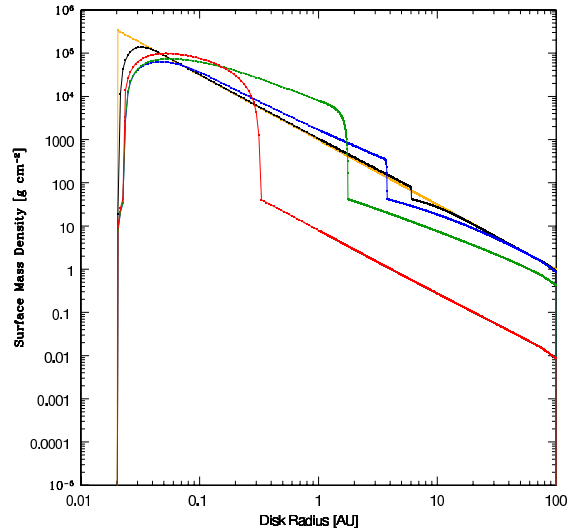


FIG. 2.— The surface mass density at $t = 0, 10^4, 10^5, 10^6,$ and 10^7 years for disk with dead zone (DZ) but no planet (RunA). The dead zone shrinks as the disk evolves.

zone (e.g. Lynden-Bell & Pringle 1974; Gammie 1996; Fromang et al. 2002):

$$\frac{dM}{dt} = 6\pi r^{1/2} \frac{\partial}{\partial r} (2\Sigma_{\text{crit}} \nu_{\text{active}} r^{1/2} + (\Sigma - 2\Sigma_{\text{crit}}) \nu_{\text{dead}} r^{1/2}), \quad (6)$$

where Σ_{crit} is the critical surface mass density below which the disk is well-ionized, while Σ is the total gas surface mass density. Specifically, we assume that the local disk is “dead” if $\Sigma > \Sigma_{\text{crit}} = 21$, and 80 g cm^{-2} for the surface mass density at 1 AU of $\Sigma_0 = 10^3$ and 10^4 g cm^{-2} , respectively. The factor of 2 in front of Σ_{crit} implies the upper and lower layers. Also, $\nu = \alpha c_s h$ is the viscosity (α is the viscosity parameter, c_s is the sound speed, and h is the disk pressure scale height), and the subscripts dead and active imply parameters in the dead zone and active layers respectively.

From the above equation, we can define the “vertically averaged” disk viscosity parameter that is weighted by the surface mass density:

$$\alpha = \frac{1}{\Sigma} (2\Sigma_{\text{crit}} \alpha_{\text{active}} + (\Sigma - 2\Sigma_{\text{crit}}) \alpha_{\text{dead}}). \quad (7)$$

In our simulations, the protoplanetary disks evolve viscously according to this viscous α .

Now we will show one example which describes a typical evolution of a disk with a dead zone. Using the averaged alpha value in Eq. 7, and assuming that $\alpha_{\text{active}} = 10^{-2}$ and $\alpha_{\text{dead}} = 10^{-5}$, we evolve a MMSN-type disk with $\Sigma = 10^3 (a/\text{AU})^{-3/2} \text{ g cm}^{-2}$ as in Fig. 2 and 3 (RunA, see Table 1 for initial conditions). Fig. 2 shows the surface mass density evolution of a disk with a dead zone, including the effect of the surface layer accretion. There is no planet in this case. An important feature of disks with dead zones is immediately apparent in this figure. The high advection speed in the outer disk, compared to the much lower speed in the region containing the dead zone, results in a pile up of gas. This manifests itself in a steep density gradient, which we have already shown can play an important role in reflecting the inwardly migrating planets in the outer disk regions (MPT07). As material accretes along the surface of the dead zone, we see that this dense front moves inward.

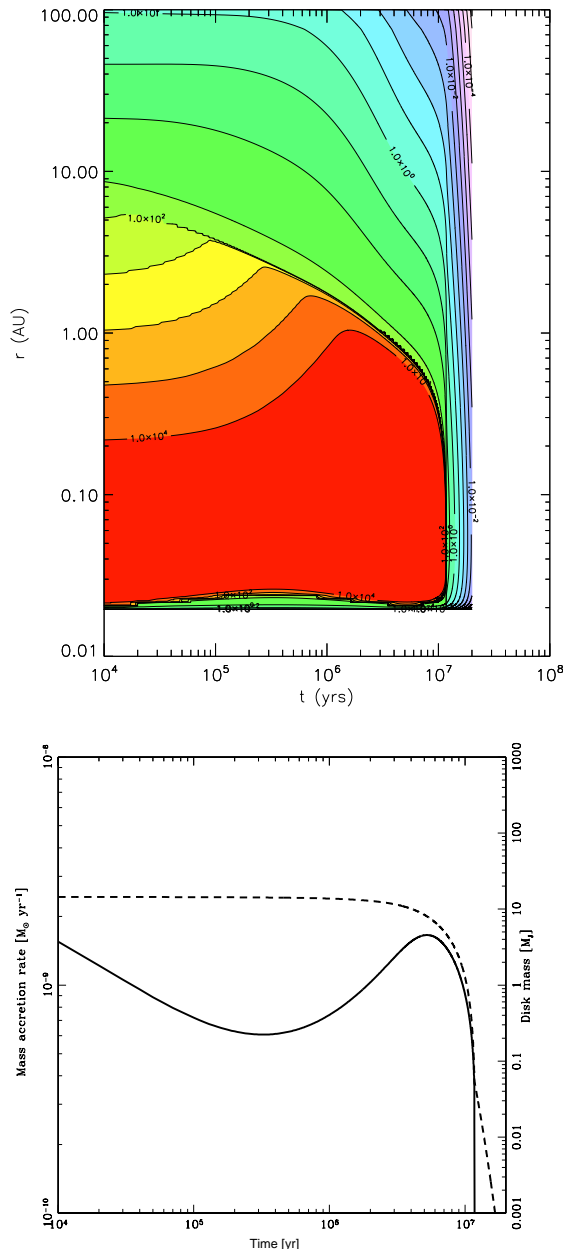


FIG. 3.— Evolution of disk with DZ but no planet (RunA) Top: Evolution of the disk column density. The disk viscosity parameter is set to $\alpha = 10^{-5}$ inside the dead zone, and 10^{-2} outside it. The dead zone shrinks rapidly due to mass accretion through the surface layers. Bottom: Corresponding plots of disk accretion rate (solid line) and disk mass (dashed line). Once the dead zone is gone, the disk disappears quickly.

The dead zone shrinks very rapidly, and only within 2 AU is dead by 2 Myr. We will see how the evolution of a dead zone affects planet formation in §5.

The corresponding figure for the disk evolution is shown in the top panel of Fig. 3. Note that the dead zone edge is where the surface mass density contours are the densest. The accretion onto the central star speeds up as the dead zone disappears. The evolution of mass accretion rate (solid line) and disk mass (dashed line) for the same run are shown in the bottom panel of Fig. 3. With a dead zone, the mass accretion rate is nearly constant for a few Myr, and more than 10% of the initial disk mass accretes onto the central star once the dead

zone is gone at around 10 Myr. This final dispersal of a disk proceeds at the viscous time scale of a turbulent disk if there is no other mechanism, and takes about a few Myr.

This characteristic evolution of the disk accretion rate in disks with dead zones may have an interesting implication for the observations. The current observations indicate that mass accretion rate is a gradually decreasing function in time (e.g. Sicilia-Aguilar et al. 2006), although the range in mass accretion rate $10^{-10} - 10^{-7} M_{\odot} \text{ yr}^{-1}$ is roughly constant between 1 – 10 Myr. In a standard disk with no dead zone, a gradual decrease of disk mass is expected (see Fig. 6 for example), and therefore we may need very massive initial disks to explain the long-lived, strong accretors.

Alternatively, if the dead zone is playing a role in disk dispersal, the mass accretion rate is likely to stay nearly constant throughout the evolution until the dead zone disappears. In this case, mass accretion rates correlate with disk masses as well as the difference between effective viscosities inside and outside the dead zones. Once the dead zone disappears, the rest of the disk accretes onto the central star at a higher viscous accretion rate. Currently, it is difficult to say whether gas accretion rates tend to decrease gradually, or stay rather constant for a significant part of the disks’ lifetime. Future observations may constrain masses and accretion rates of protoplanetary disks more precisely to indicate a possible preferred path.

2.3. Disk models

We study planet formation in a protoplanetary disk by assuming that a single planetary embryo with $0.6 M_E$ is embedded in gas and planetesimal disks. This is the same initial core mass used in P96, HBL05, and A05. In this paper, we use three slightly different gas disk models to compare our results directly with the previous studies, but keep the solid surface mass density the same $\Sigma_{solid} = 270(r/AU)^{-2}$ for all the models. Instead of choosing a specific planetesimal size, we use different planetesimal sizes ranging from 100 m to 100 km, and compare their results with one another.

In §3, we check our gas accretion prescription against P96 and HBL05, and simulate the formation of a planet on a fixed orbit in an inviscid disk. To make the comparison easier, we adopt the same initial conditions as P96 and HBL05 — the viscosity parameter is $\alpha = 0$, the gas surface mass density profile is $\Sigma_{gas} = 700(r/(5.2 AU))^{-2} = 18950(r/AU)^{-2}$, the disk temperature is $T = 150(r/5.2 AU)^{-1/2} = 342(r/AU)^{-1/2}$, and the disk extends from 0.25 to 50 AU. We use both a standard $\kappa = 1 \text{ cm}^2 \text{ g}^{-1}$ and a reduced $\kappa = 0.03 \text{ cm}^2 \text{ g}^{-1}$ opacity for our runs.

In §4, we include the effect of disk evolution and planet migration, and compare our results with A05. Again, we choose the same initial conditions as A05 to make the comparison easier, which is the same as §3 except $\alpha = 2 \times 10^{-3}$, and $\Sigma_{gas} = 525(r/(5.2 AU))^{-2} = 14196(r/AU)^{-2}$.

Finally in §5, we study the effect of a dead zone on planet migration and formation. We use the same disk model as MPT07 — $\Sigma_{gas} = \Sigma_0(r/AU)^{-3/2}$ with $\Sigma_0 = 10^3$ or 10^4 g cm^{-2} , and the disk temperature model by Robberto et al. (2002), which takes account of the effect

of a cluster environment. In this model, the disk extends from 0.02 to 100 AU. Throughout this section, we use the viscosity parameter $\alpha = 10^{-5}$ inside the dead zones, and $\alpha = 10^{-2}$ for the disk beyond it (active zones). Here, the initial value of the outer dead zone radius is ~ 8.2 , and 15.8 AU for $\Sigma_0 = 10^3$, and 10^4 g cm $^{-2}$, respectively. These values of viscosity parameter agree well with the numerical simulations done by Fleming & Stone (2003).

The initial conditions of all runs are summarized in Table 1.

3. PLANET FORMATION IN NON-EVOLVING PROTOPLANETARY DISKS

In this section, we check our gas accretion prescription against previous studies. We simulate *in situ* planet formation in a non-evolving protoplanetary disk by adopting the same initial conditions as P96 and HBL05, and compare our results with theirs. The disk models in this section assume an inviscid disk (i.e. disk viscosity parameter is $\alpha = 0$ throughout the disk) which extends from 0.25 to 50 AU (see §2.3 for details).

3.1. Effect of the planetesimal size

In this subsection, we focus on the effect of the planetesimal size on planet formation timescale. Generally speaking, smaller planetesimals lead to faster accretion because they are subject to the stronger damping of random velocities, and hence have larger cross-sections for accretion by a protoplanet.

P96 investigated the giant planet formation in a non-evolving disk, and found that a Jupiter-like planet can form *in situ* within about 8 Myr, while a similar study with an improved equation of state and opacity tables by HBL05 predicts 6 Myr. We use the same initial conditions as P96 and HBL05, and run four different simulations by changing only the planetesimal size from 100 m to 100 km (RunB1-4). RunB4 corresponds to the fiducial model in P96, and $10H\infty$ in HBL05.

Fig. 4 shows the results of our simulations of gas and planetesimal accretion by a protoplanetary core with $0.6M_E$ at a fixed orbit (5.2 AU). The top panel is the time evolution of core, envelope, and total masses of a protoplanet for a planetesimal size of 100 m, 1 km, 10 km, and 100 km from left to right. The bottom panel shows the time evolution of core and envelope mass accretion rates for the corresponding runs. Once the core accretion ceases, the transition from Eq. 2 to 3 occurs, and the envelope accretion rate increases, which is marked by a jump. Planets approach their final masses as the gas accretion slows down due to the subdisk accretion and a gap-opening.

As the previous studies have shown, we find that the core building takes longer for a swarm of larger planetesimals, and so does the time until the start of the rapid gas accretion. As it was mentioned earlier, this is because smaller planetesimals have larger accretion cross-sections by a protoplanet. For 100 m-size planetesimals, a Jupiter-like planet forms within about 2 Myr, while for 10 km-size planetesimals, it takes about 7 Myr, which is roughly the same as the time estimated for the fiducial model of P96 (~ 8 Myr) or the corresponding model ($10H\infty$) in HBL05 (~ 6 Myr).

Now we compare our results with the fiducial model of P96 and $10H\infty$ in HBL05. P96(HBL05) obtained the

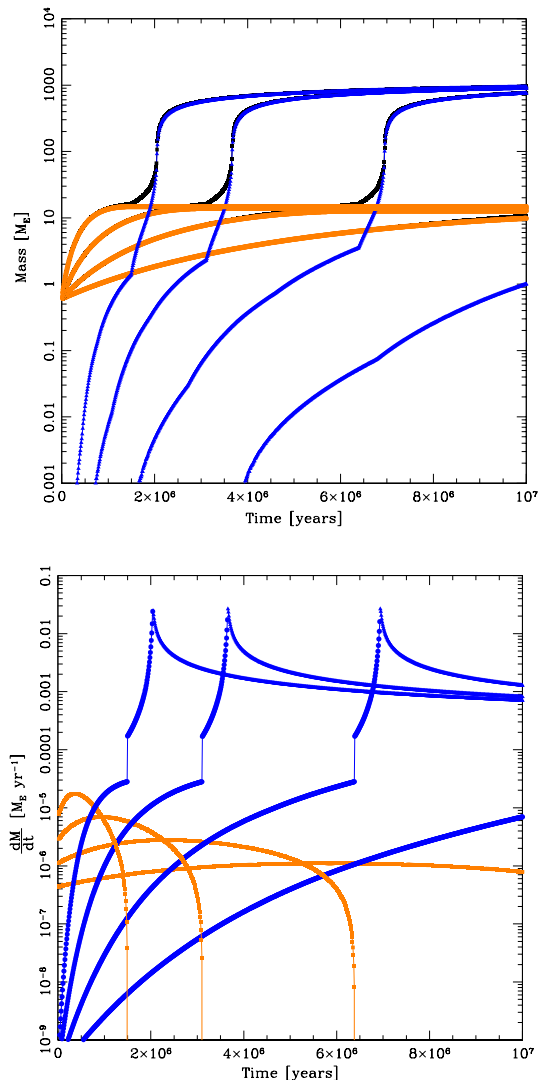


FIG. 4.— Evolution of planetary masses and accretion rates for planet at fixed disk orbital radius of 5.2 AU (RunB1-4). Top: Evolution of planetary mass which is initially $0.6M_E$. The planet has a fixed orbit at 5.2 AU from the central star. The black curves show the total masses of planets, the orange curves show the core masses, and the blue curves show the envelope masses. Different sets of curves represent planetary growth with different planetesimal sizes (100 m, 1, 10, and 100 km.) The accretion time becomes shorter for smaller planetesimals. The models with planetesimal size about 10 km produce a similar result to P96, and $10H\infty$ in HBL05. Bottom: Corresponding mass accretion rates. Orange curves are core accretion rates, and blue curves are gas accretion rates from Eq. 2, 3, and 5.

estimated formation timescale of 8(6) Myr for 100 km-size planetesimals. In our run, the corresponding case (RunB4) did not achieve a Jupiter mass within the simulation time (10 Myr). Moreover, although the mass evolution profiles look qualitatively similar to the ones in P96 or HBL05, the details appear to be different. Phase 1 and 2 in their cases are merged in our case. The difference is apparent by comparing the bottom panel of Fig. 4 with Fig. 1b in P96. In their case, rapid planetesimal accretion (Phase 1) ceases when a protoplanet depletes its planetesimal feeding zone, and this is followed by slow gas accretion (Phase 2), which lasts until the planet obtains the crossover mass for rapid gas accretion (Phase 3). Since they assume rapid planetesimal accre-

TABLE 1

INITIAL CONDITIONS FOR ALL THE RUNS. FROM LEFT TO RIGHT COLUMNS, THERE ARE RUN NAME, INITIAL GAS SURFACE MASS DENSITY ($\Sigma_{\text{gas}} = \Sigma_0(a/AU)^{-p}$ [g cm^{-2}]), DISK TEMPERATURE ($T = T_0(a/AU)^{-q}$ [K]), PLANETESIMAL SIZE, VISCOUS ALPHA VALUES IN ACTIVE AND DEAD ZONES, OPACITY, AND TORQUE SOFTENING PARAMETER.

Run	(Σ_0 [g cm^{-2}], p)	(T_0 [K], q)	planetesimal size	(α_{active} , α_{dead})	κ [$\text{cm}^2 \text{g}^{-1}$]	B
A	(10^3 , 1.5)	MPT07	N/A	(10^{-2} , 10^{-5})	N/A	N/A
B1	(1.9×10^4 , 2)	(342, 0.5)	100 m	(0, N/A)	1	N/A
B2	(1.9×10^4 , 2)	(342, 0.5)	1 km	(0, N/A)	1	N/A
B3	(1.9×10^4 , 2)	(342, 0.5)	10 km	(0, N/A)	1	N/A
B4	(1.9×10^4 , 2)	(342, 0.5)	100 km	(0, N/A)	1	N/A
C1	(1.9×10^4 , 2)	(342, 0.5)	100 m	(0, N/A)	0.03	N/A
C2	(1.9×10^4 , 2)	(342, 0.5)	1 km	(0, N/A)	0.03	N/A
C3	(1.9×10^4 , 2)	(342, 0.5)	10 km	(0, N/A)	0.03	N/A
C4	(1.9×10^4 , 2)	(342, 0.5)	100 km	(0, N/A)	0.03	N/A
D1	(1.4×10^4 , 2)	(342, 0.5)	10 km	(2×10^{-3} , N/A)	1	0.6
D2	(1.4×10^4 , 2)	(342, 0.5)	100 m	(2×10^{-3} , N/A)	1	0.6
D3	(1.4×10^4 , 2)	(342, 0.5)	100 m	(2×10^{-3} , N/A)	1	0.9
E1	(10^3 , 1.5)	MPT07	100 m	(10^{-2} , 10^{-5})	1	0.6
E2	(10^3 , 1.5)	MPT07	100 m	(10^{-2} , 10^{-5})	0.03	0.6
F1	(10^4 , 1.5)	MPT07	100 m	(10^{-2} , 10^{-5})	1	0.6
F2	(10^4 , 1.5)	MPT07	100 m	(10^{-2} , 10^{-5})	0.03	0.6
G1, & G2	(10^3 , 1.5)	MPT07	100 m	(10^{-2} , 10^{-5})	0.03	0.6
H1	(10^4 , 1.5)	MPT07	100 m	(10^{-2} , 10^{-5})	0.03	0.6
H2	(10^4 , 1.5)	MPT07	100 m	(10^{-2} , 10^{-5})	1	0.6

tion, the planetesimal accretion rate is very high during Phase 1 ($dM/dt \sim 10^{-4} - 10^{-2} M_E/\text{yr}$), and drops to $\sim 10^{-6} M_{\text{EYR}}^{-1}$ during Phase 2 due to planetesimal depletion in the feeding zone (see Fig. 1b of P96.) Their protoplanetary core grows from $0.6M_E$ to $\sim 10M_E$ during Phase 1 (within 0.5 Myr).

However, as we mention in §2, protoplanets more massive than a few times $10^{-5}M_E$ are expected to grow *oligarchically*. In our simulations, since we assume slower, oligarchic growth from the start, the planetesimal accretion rate is low all the time $\sim 10^{-5} - 10^{-6} M_{\text{EYR}}^{-1}$ and drops to zero once the planetesimals are depleted. As a result, the core mass does not reach $\sim 10M_E$ for a few Myr in RunB3. The difference in core growth prescription may not seem to have a significant effect on a non-migrating planet in the inviscid disk, but becomes important for a migrating planet in an evolving disk. We discuss this further in §4 and 5.

3.2. Effect of the opacity

A reduced opacity in the gaseous envelope of a protoplanet can lead to the faster gas accretion (P96 and INE00). HBL05 extended the work of P96, and studied the effects of disk's opacity as well as a planetary core mass. By assuming 2% of the opacity of interstellar grains, they found that the gas accretion time becomes significantly shorter (1–4.5 Myr). This effect is reflected in the gas accretion timescale we adopt (see Eq. 2 and 3).

We keep the definition of our solid surface mass density, and change the size of planetesimals from 100 m to 100 km as in the last subsection (RunC1-4). RunC4 corresponds to the model of $10L_\infty$ in HBL05. Here, we adopt a reduced, constant opacity of $\kappa = 0.03 \text{ cm}^2 \text{ g}^{-1}$, which is an average opacity value obtained for the model $10L_\infty$ in HBL05 over a relevant range of temperature of protoplanetary disks (roughly 100 – 1000 K).

The results of our simulations are shown in Fig. 5. Comparing Fig. 4 with 5, we confirm that the lower opacity results in the faster gas accretion. HBL05 showed that

the formation time could be as short as 2 Myr in a disk with 100 km planetesimals with a reduction in opacity (see their Fig. 1). In our simulations, a similar time scale to their model is obtained for a 10 km-size planetesimal disk (RunC3), where formation takes about 3 Myr. This is more than twice faster than our corresponding run in §3.1 with the standard opacity (RunB3). The formation time scales for our 10 km planetesimal disk models are about 1 Myr longer than those of corresponding models in HBL05 with a 100 km-size planetesimal disk ($10L_\infty$ and $10H_\infty$). Thus, our gas accretion prescription agrees fairly well with previous studies like P96 and HBL05.

4. PLANET FORMATION IN AN EVOLVING DISK

We now add disk evolution and planet migration to the formation model described in the previous section, and study their effects on planet formation to compare the results with A05. In this section of the paper, the disk viscosity parameter is assumed to be constant ($\alpha = 2 \times 10^{-3}$) throughout the disk. Therefore, different from the previous section, a protoplanetary disk accretes toward the central star. Note that this model does not include a dead zone. The other initial conditions of the disk models are explained in §2.3, and summarized in Table 1.

A05 adopted the migration speed obtained by Tanaka et al. (2002), and reduced the migration rate artificially by a factor of 0.1–0.01. To incorporate the idea, but to keep the generality, we use the torque expression presented by Menou & Goodman (2004), and adjust the softening parameter B , which mimics the torque reduction effect with a vertical height (also see Appendix B in MPT07).

First, we show our fiducial migration case with $B = 0.6$, which roughly corresponds to the migration speed estimated by Tanaka et al. (2002). Fig. 6 shows the growth of a planet with an initial mass of $0.6M_E$ in a 10 km-size planetesimal disk (RunD1). The planetesimal accretion is very slow as it can be seen in the bottom panel, and therefore the protoplanet does not migrate

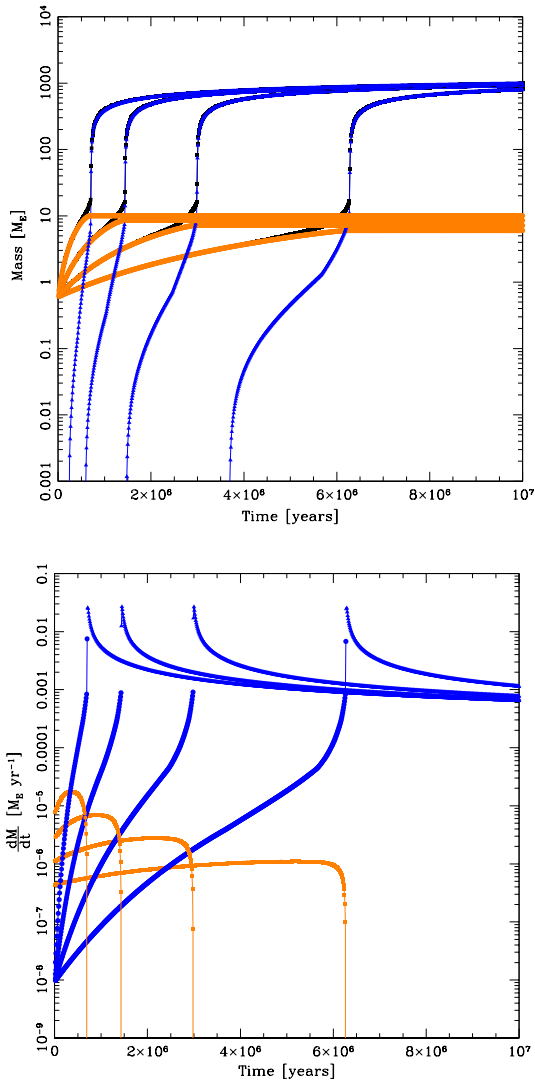


FIG. 5.— Effect of reduced opacity on evolution of planetary masses and accretion rates for planet at fixed orbital radius of 5.2 AU (RunC1-4). Top: The same as Fig. 4, but with a disk opacity of $\kappa = 0.03 \text{ cm}^2 \text{ g}^{-1}$. The model with planetesimal size about 10 km results in a similar outcome to the model 10L ∞ in HBL05. Bottom: Corresponding mass accretion rates.

much. The final mass is about $1 M_E$, only barely increased from $0.6 M_E$. Also plotted in the bottom panel of Fig. 6 are the disk mass evolution (dashed line) and disk accretion rate onto the central star (solid thin line). It is interesting to compare this figure with the disk evolution with a dead zone (see the bottom panel of Fig. 3). Viscous disk accretion rate, and hence disk mass, decrease gradually rather than being nearly constant over a long time as in the case with a dead zone. If all disks have high alpha values $\alpha > 10^{-3}$, very massive disks may be necessary to explain the existence of long-lived, strong accretors.

Fig. 7 shows the same run as Fig. 6, but with the planetesimal size of 100 m (RunD2). The planet migrates inward, and plunges into the central star within about 2 Myr. Although the planetary mass increases rapidly as the protoplanet migrates, the final mass is about $15 M_E$, and there is little gas accretion. Although the final gas accretion rate becomes comparable to the solid accretion

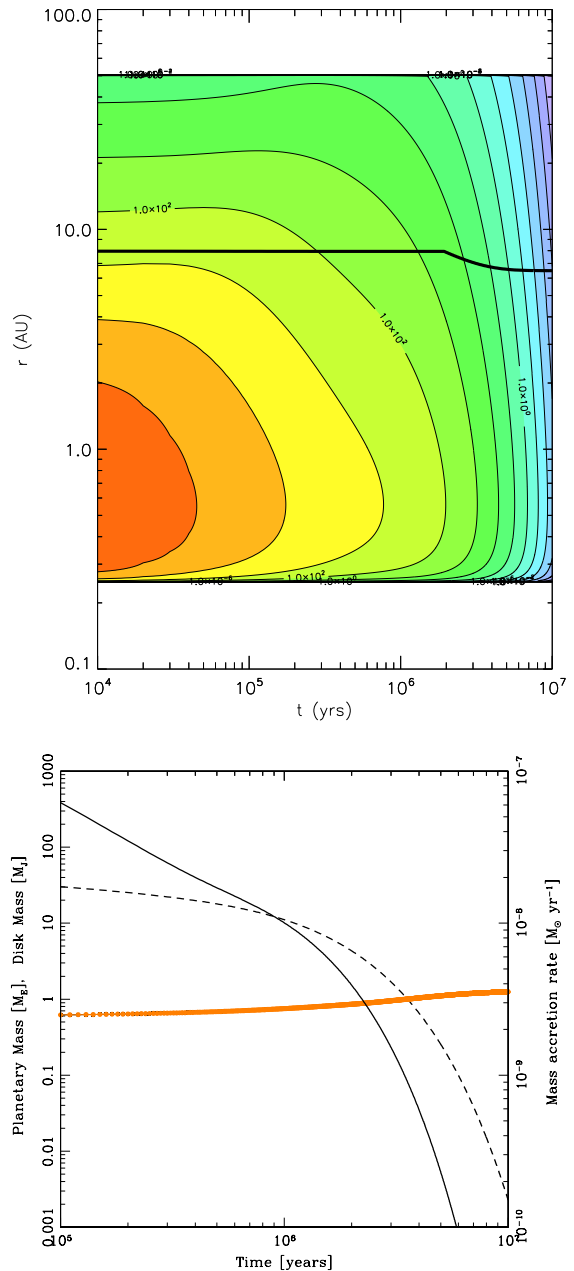


FIG. 6.— Evolution of planet and disk for planetesimal sizes of 10 km and no DZ (RunD1). Top: Evolution of a planet with an initial mass of $0.6 M_E$ in an evolving disk with no dead zone. The disk viscosity parameter is set to $\alpha = 2 \times 10^{-3}$, and the planetesimal size is 10 km. We use our fiducial softening parameter $B = 0.6$. There is very little growth of a planet, and as a result, the planet does not migrate much. Bottom: Corresponding evolution of planet and disk masses as well as disk accretion rate onto the star. Solid, and dashed curve shows disk accretion rate, and disk mass, respectively. Thick orange, and black curves are on top of each other, and show core, and total planetary mass, respectively.

rate ($\sim 5 \times 10^{-5} M_E \text{ yr}^{-1}$), migration is too fast in this case to make a Jupiter-like planet. It should be noted, however, that the resolution of our simulation is good down to 0.1 AU, and that we don't define the inner dead zone edge. Therefore, any planets which appear to be “lost” in our simulations may still be alive if we improve our resolution, take account of the inner dead zone edge, or include the star-planet tidal interaction.

Now we show the case of slower migration by adopting a larger softening parameter of $B = 0.9$ (RunD3), which

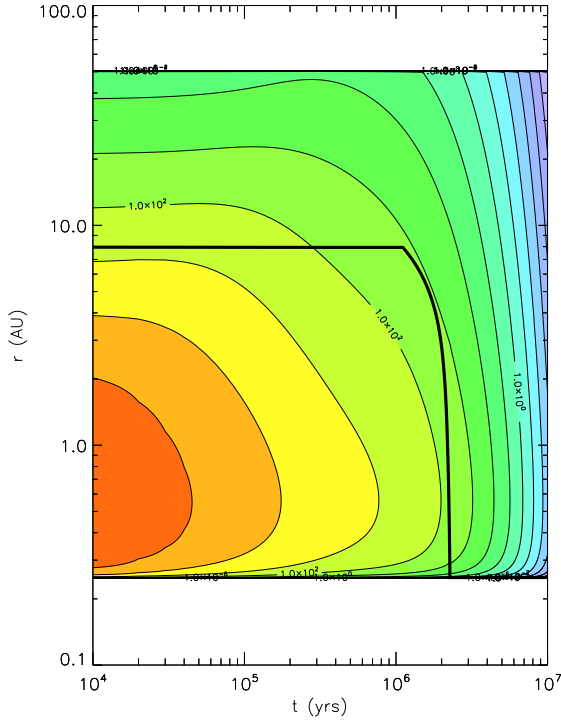


FIG. 7.— Evolution of planet and disk with no DZ (as in Fig. 6), except with planetesimal sizes of 100 m (RunD2). Top: The protoplanet plunges into the star within 2 Myr, and its final mass is roughly $20 M_E$. Bottom: Corresponding evolution of planet and disk masses as well as the disk accretion rate onto the star.

roughly reproduces the migration profile of A05 (see their §3.1.) Fig. 8 shows such an evolution in a disk with 100 m-size planetesimals. The planet migrates more slowly, but grows only up to $\sim 10 M_E$. From disk mass evolution (dotted line on the bottom panel), we can see that formation of a Jupiter mass planet is impossible after 4 Myr, since the disk mass falls below M_J . In our run, the planet’s mass is $\sim 7 M_E$ at 4 Myr.

This is very different from what A05 obtained, where the planet starts opening a gap after 0.8 Myr at around 6 AU, and stops its migration at around 5.5 AU. This results from the difference in solid accretion prescriptions as described briefly in the previous section. A05 followed P96 and adopted rapid planetesimal accretion for the growth of the planetary core with an initial mass

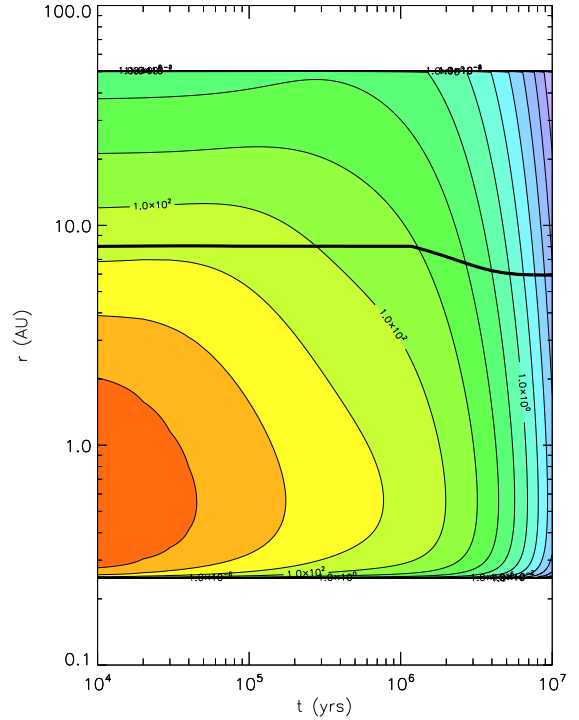


FIG. 8.— Evolution of planet and disk for planetesimal sizes of 100 m and no DZ, but with larger softening parameter $B = 0.9$ (RunD3). The planet migrates much slower, but grows only up to $9 M_E$.

of $0.6 M_E$. Therefore, their core mass reaches several M_E by 0.8 Myr, while our core mass is about $2 M_E$ at that time.

In P96, the planetesimal accretion slows when the protoplanet depletes the planetesimal feeding zone. Therefore, during Phase 2, their planetary mass increases at the gas accretion rate, which is much smaller than the planetesimal accretion rate in Phase 1. As a result, the planet formation timescale in P96 was uncomfortably long. A05 overcame this problem by constantly replenishing the planetary feeding zone due to migration, and therefore increasing the total mass of a planet at the rapid planetesimal accretion rate rather than the gas accretion rate. Thus, the planet accretes gas much quicker in their case. On the other hand, Fig. 9 shows that the

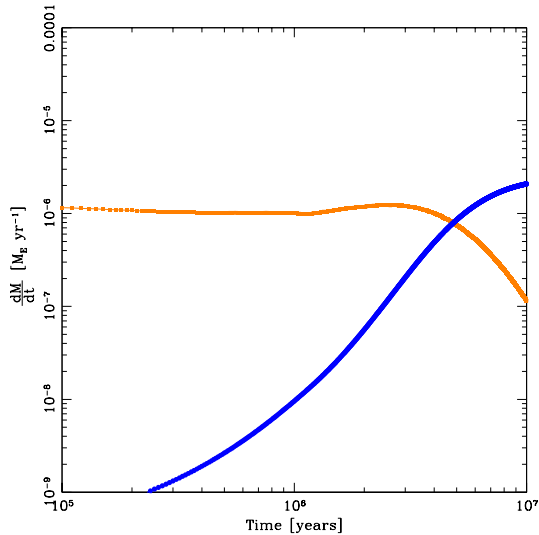


FIG. 9.— Corresponding mass accretion rate for Fig. 8. Orange curve is the core accretion rate, and blue curve is the envelope accretion rate. As the planetary mass grows, gas accretion rate increases and the two accretion rates become comparable to each other.

planetesimal accretion rate in our model is a few orders of magnitude lower than that during Phase 1 in P96, and comparable to that during Phase 2 in P96. Gas accretion rate is even smaller, or at most comparable to planetesimal accretion rate throughout the simulation. Therefore, in our case, a protoplanet increases its mass on nearly constant time scale all the time, independent of whether it is migrating or not. In short, for the *oligarchic* core accretion process, we find that the replenishment of the planetesimal feeding zone due to migration does not help planetary growth as much as it was shown by A05.

5. PLANET FORMATION IN AN EVOLVING DISK WITH A DEAD ZONE

In this section, we combine all of the elements of protoplanetary accretion and disk evolution presented above with the dead zone.

5.1. Without planet migration

First, we study the case with no migration, but with disk evolution. This, of course, is an unlikely scenario, because a growing planetary core would quickly migrate toward the central star, especially inside the dead zone due to an enhanced disk mass (see MPT07). We show these cases nevertheless, since they provide reasonable estimates of planetary masses achievable in our fiducial disks.

Fig. 10 and 11 show the results of $\Sigma_0 = 10^3$ and 10^4 g cm^{-2} respectively with standard (top panels) and reduced (bottom panels) opacities (see §2.3 and Table 1 for initial conditions for RunE1(2), and RunF1(2)). The core has an initial mass of $0.6M_E$ as before, and stays at 5 AU throughout the simulations. The planetesimal size is 100 m. In all of these cases, the protoplanetary core is originally inside the dead zone, and is left outside it as the disk grows and the dead zone shrinks. The final planetary mass of the case with a massive disk and a reduced opacity (bottom panel of Fig. 11) is about half a Jupiter mass, while all the other cases produce planets about a Neptune mass ($20M_E$). Note that in both

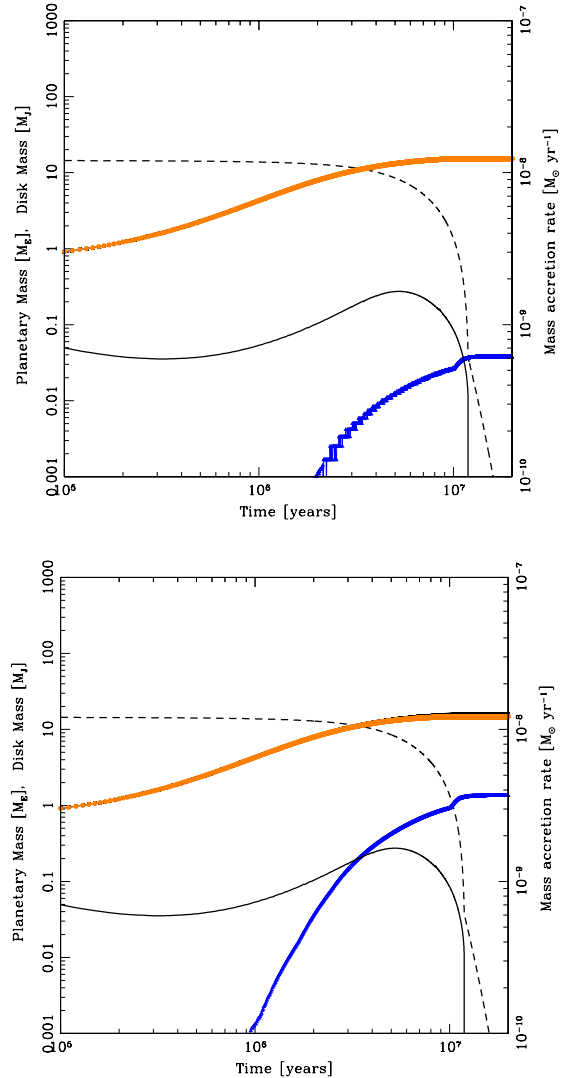


FIG. 10.— Evolution of disk mass and accretion rate, in presence of a DZ, and $\Sigma_0 = 10^3$ g cm^{-2} , with standard opacity (top panel, RunE1) and reduced opacity (bottom panel, RunE2). Also plotted are disk mass evolution (dashed curves) along with the disk accretion rate onto the central star (thin solid curves.)

MMSN-mass and more massive disks, the opacity reduction leads to more efficient gas accretion as seen in §3.2. These results further emphasize the importance of the opacity reduction in helping rapid planet formation, and indicate that it is difficult to form a Jupiter mass planet in a MMSN-mass disk.

Also plotted in Fig. 10 and 11 are evolution of disk mass (dashed lines) and disk accretion rate onto the central star (thin solid lines.) As shown in §2.2, a dead zone enforces a nearly constant accretion rate onto the star, and a rapid dispersal of a disk once it's gone.

5.2. With planet migration

Now, we finally show the cases with planetary formation and migration in an evolving disk with a dead zone. The initial conditions are the same as the previous subsection, except that planetary migration is allowed with our fiducial softening parameter $B = 0.6$.

In Fig. 12, and 13, we show the evolution of a planetary core initially at 8, and 10 AU in a MMSN-like disk

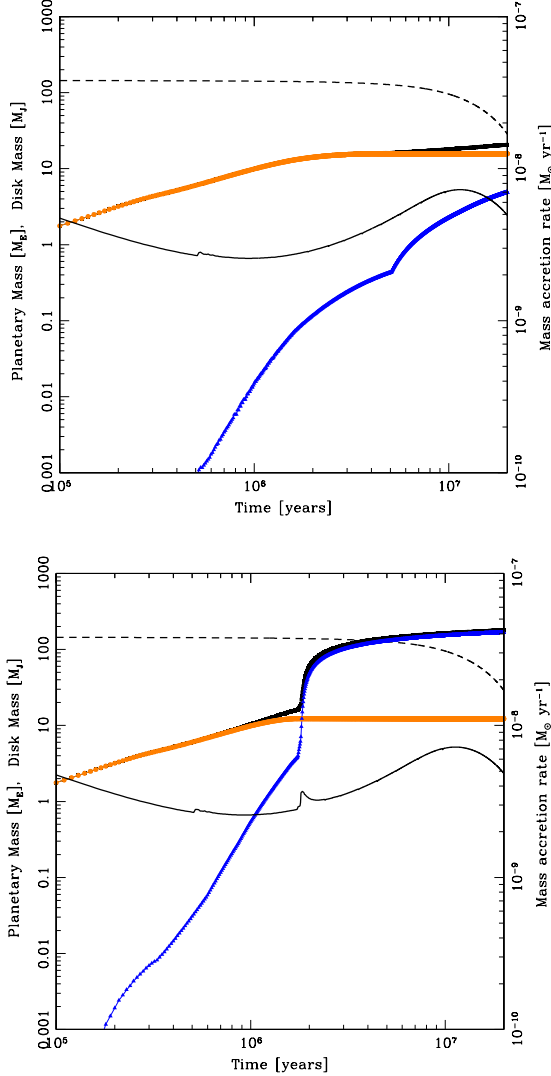


FIG. 11.— Evolution of disk mass and accretion rate (as in Fig. 10, except for column density $\Sigma_0 = 10^4 \text{ g cm}^{-2}$, with standard (top panel, RunF1) and reduced (bottom panel, RunF2) opacity.

with $\Sigma_0 = 10^3 \text{ g cm}^{-2}$, by assuming a reduced opacity and a 100 m-size planetesimal disk (RunG1 and G2, respectively). Since the initial outer dead zone radius is 8.2 AU, the protoplanet starts inside(outside) the dead zone in RunG1(G2). Note that, in Fig. 12 (RunG1), the protoplanet appears as if it were initially outside the dead zone, because the time axis is logarithmic and starts at 10^5 yr . In this case, the protoplanet is originally located inside the dead zone, but is left outside it as the dead zone shrinks over time.

The core building phase takes longer as the initial orbital radius moves outward, and as a result, the outer planet accretes less amount of gas. As expected from §5.1, neither case leads to a gas giant. Final masses are $20M_E$ for 8 AU case (RunG1), and $7M_E$ for 10 AU case (RunG2). In RunG2, the core accretion is so slow that the planet barely migrates compared to RunG1. We obtain a similar result to RunG1 for an initial radius just outside the dead zone at 9 AU.

From the comparison of Fig. 12 with Fig. 7, the effect of a dead zone is apparent. Instead of losing a growing

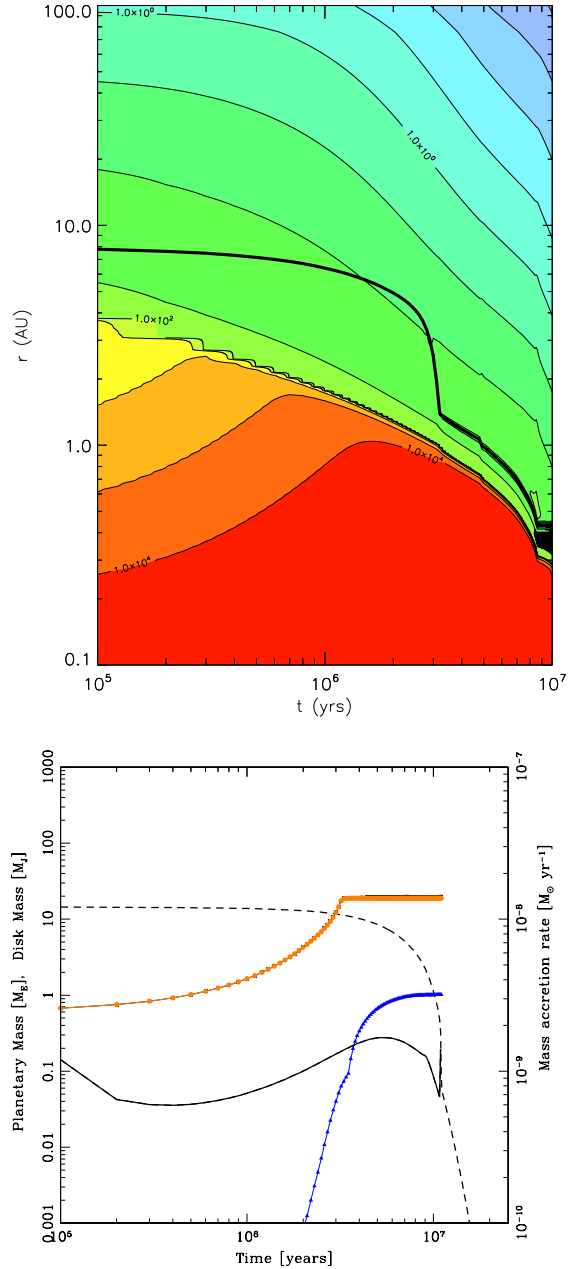


FIG. 12.— Evolution of planet and disk with a planetary core initially just inside DZ at 8 AU. The disk column density $\Sigma_0 = 10^3 \text{ g cm}^{-2}$, reduced opacity, and a 100 m-size planetesimal disk are assumed (RunG1). Top: Evolution of both disk and planetary orbital radius. Note that the planet appears as if it were initially outside the DZ, because the time axis is logarithmic and starts at 10^5 yr . Bottom: Corresponding evolution of planetary and disk masses as well as the disk accretion rate onto the central star.

protoplanet to the central star, the dead zone stops the migration of the protoplanet by balancing the inner and outer torques. As a result, the protoplanet has a chance of growing further at a slower, viscous accretion rate of the disk.

Fig. 14, and 15 show the evolution of a planetary core initially at 15 AU in a more massive disk with $\Sigma_0 = 10^4 \text{ g cm}^{-2}$, by assuming a reduced (RunH1), and a standard (RunH2) opacity, respectively. For both cases, a 100 m-size planetesimal disk is used. Since the initial outer dead zone radius is 15.8 AU, these planets start just *inside* the dead zone. However, the protoplanets

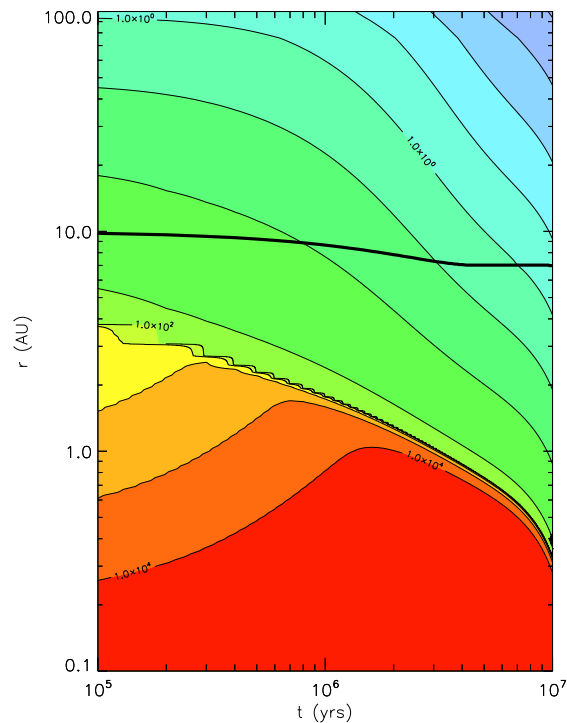


FIG. 13.— Evolution of planet and disk as in Fig. 12, except the initial orbital radius of a planet is outside DZ at 10 AU (RunG2).

appear as if they were initially outside the dead zone, because the time axis is logarithmic and starts at 10^5 yr. Run H1 obtains a gas giant with $\sim 0.3M_J$ in roughly 2.5 Myr, while in Run H2, the protoplanet grows only up to $\sim 20M_E$. This demonstrates that we need an opacity reduction (or some other mechanism) even when we include planet migration. As emphasized in §4, this is the result of a slower oligarchic core accretion compared to a runaway core accretion. The overall mass accretion onto a protoplanet does not speed up as a result of migration, and hence the constant replenishment of the planetesimal feeding zone.

Also, by comparing the bottom panels of Fig. 14 and 15, it appears that a gap-opening planet speeds up the dispersal of a gas disk. This additional disk dispersal mechanism should be investigated in multiple planet formation models.

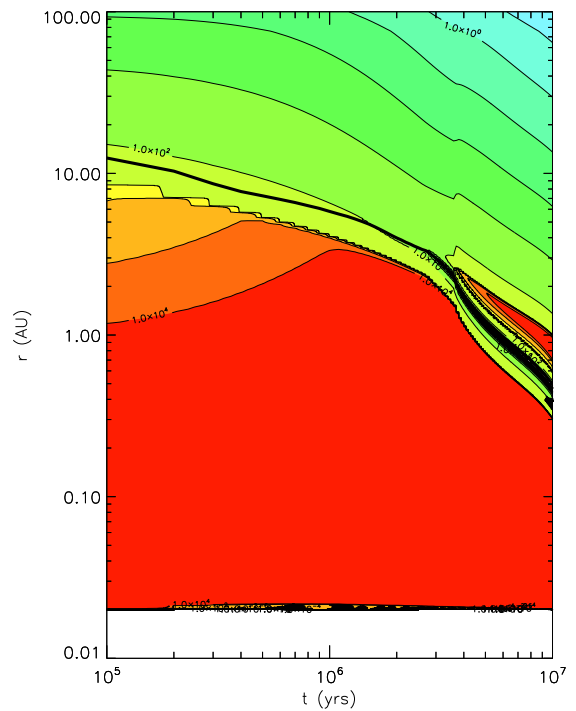


FIG. 14.— Evolution of planet and disk as in Fig. 12, except disk column density of $\Sigma_0 = 10^4 \text{ g cm}^{-2}$, and the initial orbital radius of a planet just inside DZ at 15 AU (RunH1). Note that the protoplanet appears as if it were initially outside the DZ, because the time axis is logarithmic and starts at 10^5 yr. The second jump in mass seen on the bottom panel occurs at semi-major axis smaller than our resolution limit, and may not represent the true evolution of the planet.

6. DISCUSSION AND CONCLUSIONS

We have presented some new results on planet formation and migration in evolving disks with dead zones. The most significant is that dead zones provide a natural way of saving planetary systems even as the planets migrate through disks whose properties change significantly over hundreds of thousands to millions of years. The dissipation of the disk does place interesting constraints on their masses - we find that only Neptunian mass planets can be formed in the MMSN-mass disk models. Jovian planet formation requires more massive disks, which has also been suggested by other groups (e.g. P96

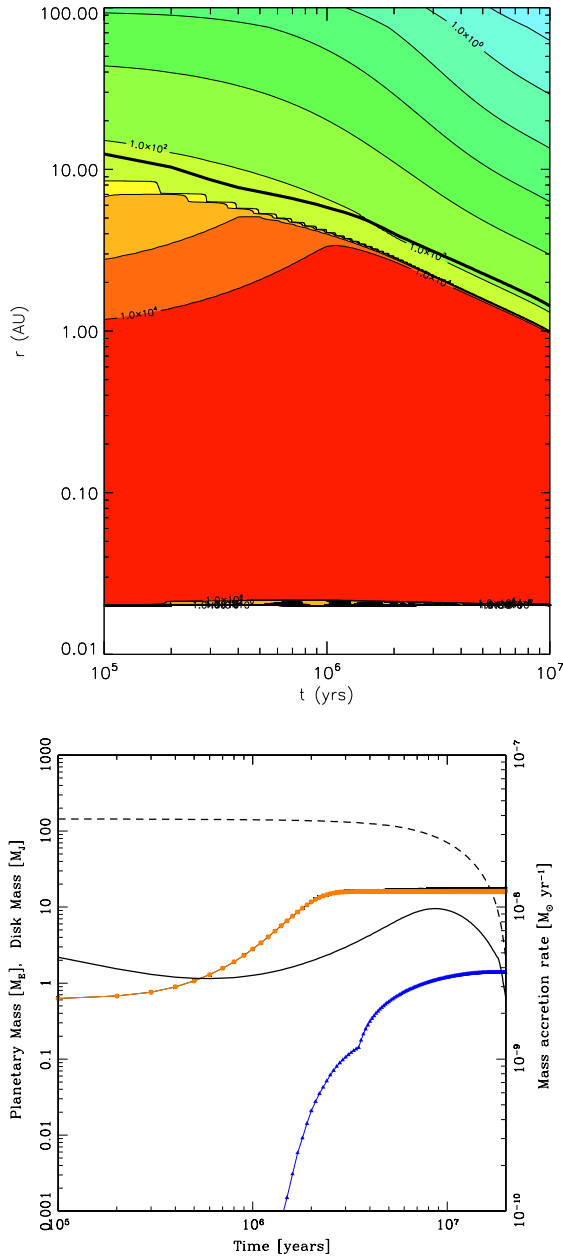


FIG. 15.— Evolution of planet and disk as in Fig. 14, but the standard opacity instead of reduced opacity is assumed (RunH2). Again, although the initial protoplanetary radius is just inside DZ at 15 AU, the protoplanet appears as if it were initially outside the DZ, because the time axis is logarithmic and starts at 10^5 yr.

and HBL05), and was recently demonstrated by multiple planet formation simulations by Thommes et al. (2008). The time scale that we find for Jovian planet formation in these more massive disks - about 2.5 Myr - is within observational limits of disk lifetimes. While not drastically reduced from previous estimates, our Jovian planet formation time incorporates many new aspects including migration in the presence of dead zones, effects of slower oligarchic growth that are more realistic than earlier accretion scenarios, and an effect of a reduced opacity.

Dead zones turn out to play a potentially important role as blockades against inward planetary motion. Our planetary cores are generally kept outside of the dead zone - and therefore immersed in the region where they can “feed” more effectively on surrounding gas. When

the planets become massive enough to open a gap, the outwards directed torque associated with the density gradient of the outer edge of the dead zone weakens, and the planets migrate into the dead zone. Planets migrate slowly inside the dead zone due to the lower viscosity there compared to outside it.

The methods we used were straightforward to implement in our planetary/disk evolution code. In order to model dead zone evolution, we simply assumed that the dead zone is where the surface mass density is above the critical value ($\Sigma > \Sigma_{crit} = 21$, and 80 g cm^{-2} for $\Sigma_0 = 10^3$ and 10^4 g cm^{-2} respectively) that was determined from a stationary disk model in MP06. Also, we have included gas accretion through the surface layers, which contributes to make a dead zone shrink very rapidly (see Fig. 3). Combining these two conditions, we have found that the dead zone radius shrinks from 8.2 AU to 2 AU within 2 Myr for $\Sigma_0 = 10^3 \text{ g cm}^{-2}$.

For the planet formation part of the code, we follow the approach by P96, but with a few differences. First of all, we assume that the planetesimal accretion stage is mainly carried out by oligarchic growth, rather than by rapid runaway accretion used by P96. This is a reasonable assumption since the runaway growth most likely ceases long before the planetary mass reaches a few times $10^{-5} M_E$ (Thommes et al. 2003), which is much smaller than our initial planetary mass ($0.6 M_E$), and switches to a slower oligarchic growth (Ida & Makino 1993; Kokubo & Ida 1998). Depending on the size distribution of planetesimals, the rate of accretion could be significantly different. Secondly, we parameterize our gas accretion rate following INE00 and D’Angelo et al. (2003). Therefore, we are not calculating planetesimal and gas accretion rates in an interactive way as in P96, HBL05, or A05. However, our simulations show reasonable agreements with their results (see §3). Also, since we take account of the subdisk accretion phase, the final stage of gas accretion slows down, rather than exponentially increases as in P96, or artificially cuts off as in HBL05. Thirdly, we include a 1D gas disk evolution and planet migration. Our approach is similar to A05, but we don’t include photoevaporation effects for this study, since this is likely to be negligible during planet formation.

There are several aspects of planet formation that we have not included explicitly in this study. We list several below, but note that we do not expect their absence to strongly affect our results.

First of all, our simple torque prescription does not capture the nature of a turbulent disk properly. A number of numerical simulations have shown that turbulent fluctuations can cause torque fluctuations (e.g. Laughlin et al. 2004; Nelson & Papaloizou 2004), which leads to stochastic type I migration (Johnson et al. 2006). This results in even *faster* migration for most planets, but also allows *outward* migration for some of them (Johnson et al. 2006). The inclusion of such an effect may allow a planet outside the dead zone to “jump the barrier” provided by the edge of a dead zone. Even within a dead zone, turbulent fluctuations in upper and lower active layers may be able to affect planet migration significantly.

Also, we do not take account of the evolution of temperature profile of a gas disk. To better evaluate the disk

evolution, we should include the radiative transfer to the code. This would affect not only the dead zone and disk evolution, but also planet migration. A recent work of Paardekooper & Mellema (2008) demonstrated that, in a non-isothermal disk, planet migration is preferentially outward at around 5 AU until the disk mass decreases significantly. Therefore, more precise treatment of a disk temperature may save type-I migrators effectively, even inside a dead zone.

Perhaps the most important simplification of our model is the 1D treatment of the disk, and the rather crude prescriptions for the dead zone, which led to a very sharp density transition at the outer dead zone radius (see Fig. 2). This feature enabled a planet to stop its migration by balancing inner and outer torques. However, such a sharp density gradient makes a disk locally Rayleigh unstable (i.e. an epicyclic frequency $\kappa^2 < 0$), which may render the sharp transition from the dead zone to the outer active disk much smoother. Even when the disk is still locally stable, the Rossby wave instability can smooth the density gradient in a similar manner when pressure varies significantly over a few times the disk thickness (Li et al. 2001, and the references therein). This possibility should be checked carefully by numerical simulations.

We did not take account of the effect of the corotation torque either. This is a safe assumption most of the time, since the corotation torque depends on the gradient of the inverse of the specific vorticity ($\partial(\Sigma/B)/\partial r$) (Goldreich & Tremaine 1980; Masset 2001), and therefore its effect becomes particularly important when the surface mass density changes sharply, e.g. at the edge of a dead zone. However, we do not expect this affects our results significantly, because inner and outer Lindblad torques balance with each other far away from the density jump, where the corotation torque is likely negligible, and planet migration stalls (also see Appendix B in MPT07). When Rayleigh, or Rossby wave instability makes the density gradient at the outer edge of a dead zone smoother, the corotation torque can become important. In such a case, a planet would not be stopped at the outer edge of a dead zone, but pulled into it instead.

The corotation torque is also found to be important for migration of sub-Jovian mass planets like Saturn (Masset & Papaloizou 2003). In a standard disk, the time scale of the so-called type III migration for such planets is comparable to, or even shorter than, type I migration (Masset & Papaloizou 2003). Although this is most relevant to our RunH1 (Fig. 14), we don't expect a significant change in our result. This is because type III migration is likely to switch to slower type II migration as soon as the planet enters a dead zone, where planets tend to open a wider gap at smaller mass due to its low viscosity.

Another simplifications is that we have only considered a protoplanetary disk with a single core, while the real disks are expected to have multiple cores. Studies of this kind have been done by Chambers (2006); Thommes et al. (2008) for disks with no dead zone, and by Morbidelli et al. (2008) at the *inner* edges of disks with dead zones. A recent paper by Ida & Lin (2008), took a similar approach to us, and studied a dead zone's effects on retaining icy grains, as well as protoplanetary cores. They reproduced the observed frequency

and mass-period distribution of gas giants around solar-type stars with a moderate reduction in type I migration speed.

Yet another simplification is that all of our planets in this study are on circular orbits. Planet-disk interaction has been proposed as a method to drive planetary eccentricity (Goldreich & Sari 2003), and recent numerical simulations confirmed this for massive ($> M_J$) planets (e.g. Masset & Ogilvie 2004; D'Angelo et al. 2006). If a planetary eccentricity is enhanced significantly ($e \gg h/r$), then planet migration could be slowed down (e.g. Papaloizou & Larwood 2000; Papaloizou 2002), and mass growth rate could increase (e.g. D'Angelo et al. 2006; Kley & Dirksen 2006).

We also employ simplified planetesimal disks. First, we only consider single-size planetesimals ranging from 100 m to 100 km, while the real disks should have multiple-size planetesimals. Secondly, we don't include the planetesimals' effect on planet migration, which could potentially be important (Murray et al. 1998). Thirdly, we assume the dispersion-dominated random velocities for planetesimals with all sizes. Since small planetesimals experience strong gas drag and achieve reduced random velocities, their mass accretion rate should be treated in the shear-dominated regime (Rafikov 2004; Chambers 2006). This may be important for 100 m-size planetesimals (Chambers 2006), and the planetesimal accretion would be runaway, rather than oligarchic in such a case.

Finally, we don't include the effects of photoevaporation (e.g. Shu et al. 1993; Hollenbach et al. 1994), which is likely to be important during the last stage of disk evolution (Clarke et al. 2001; Alexander et al. 2006). However, photoevaporation becomes important only when disk mass becomes significantly low ($\sim 1M_J$ or so), and therefore it is unlikely to affect our results.

We conclude by listing our major findings:

- (1) Dead zones strongly evolve over the duration of the disk, starting with outer radii of order 10 – 15 AU, and shrinking with time to of order an AU or less.
- (2) Protoplanets which are left outside the dead zone tend to migrate inward as they accrete planetesimals, and stop just outside the outer dead zone radius due to a steep surface mass density jump. Then such protoplanets migrate at the viscous time scale of the shrinking dead zone until they achieve gap-opening mass. Once they open a gap, they enter the dead zone, and migrate inwards rather slowly due to the low viscosity there.
- (3) The final mass of a planet is determined by disk mass. In a minimum-mass solar nebula disk, it is difficult to get a planet more massive than Neptune. We find Jovian planets form in disks that are ten times more massive than this.
- (4) A Jupiter mass planet can form within ~ 2.5 Myr (see Fig. 14) in a disk with a dead zone, by assuming standard type I migration. However, since planet migration does not help core accretion as much in oligarchic growth as in runaway growth scenario, we expect that the opacity reduction (or some other mechanism) is necessary to form a Jovian planet within a disk life time.

(5) Dead zones may help explain the existence of long-lived strong accretors. When a dead zone is present, the mass accretion rate is likely to take a nearly constant value until the dead zone disappears, rather than decreasing gradually as expected in a standard disk without a dead zone. Once this happens, the rest of the disk is dispersed on a few Myr time scale, unless photoevaporation and/or planet formation provide additional sources of disk dissipation.

ACKNOWLEDGMENTS

REFERENCES

- Alexander, R. D., Clarke, C. J., & Pringle, J. E. 2006, *MNRAS*, 369, 229
- Alibert, Y., Mordasini, C., Benz, W., & Winisdoerffer, C. 2005, *A&A*, 434, 343
- Andrews, S. M. & Williams, J. P. 2005, *ApJ*, 631, 1134
- Balbus, S. A. & Hawley, J. F. 1991, *ApJ*, 376, 214
- Bate, M. R., Lubow, S. H., Ogilvie, G. I., & Miller, K. A. 2003, *MNRAS*, 341, 213
- Boss, A. P. 1997, *Science*, 276, 1836
- Bryden, G., Chen, X., Lin, D. N. C., Nelson, R. P., & Papaloizou, J. C. B. 1999, *ApJ*, 514, 344
- Chambers, J. E. 2006, *ApJL*, 652, L133
- Clarke, C. J., Gendrin, A., & Sotomayor, M. 2001, *MNRAS*, 328, 485
- Cuzzi, J. N., Dobrovolskis, A. R., & Champney, J. M. 1993, *Icarus*, 106, 102
- D'Angelo, G., Henning, T., & Kley, W. 2002, *A&A*, 385, 647
- D'Angelo, G., Kley, W., & Henning, T. 2003, *ApJ*, 586, 540
- D'Angelo, G., Lubow, S. H., & Bate, M. R. 2006, *ApJ*, 652, 1698
- Duncan, M. J., Levison, H. F., & Lee, M. H. 1998, *AJ*, 116, 2067
- Fleming, T. & Stone, J. M. 2003, *ApJ*, 585, 908
- Fromang, S., Terquem, C., & Balbus, S. A. 2002, *MNRAS*, 329, 18
- Gammie, C. F. 1996, *ApJ*, 457, 355
- Glassgold, A. E., Najita, J., & Igea, J. 1997, *ApJ*, 480, 344
- Goldreich, P. & Sari, R. 2003, *ApJ*, 585, 1024
- Goldreich, P. & Tremaine, S. 1980, *ApJ*, 241, 425
- Goldreich, P. & Ward, W. R. 1973, *ApJ*, 183, 1051
- Hartmann, L., Calvet, N., Gullbring, E., & D'Alessio, P. 1998, *ApJ*, 495, 385
- Hollenbach, D., Johnstone, D., Lizano, S., & Shu, F. 1994, *ApJ*, 428, 654
- Hubickyj, O., Bodenheimer, P., & Lissauer, J. J. 2005, *Icarus*, 179, 415
- Hueso, R. & Guillot, T. 2005, *A&A*, 442, 703
- Ida, S. & Lin, D. N. C. 2008, *ArXiv e-prints*, 802
- Ida, S. & Makino, J. 1993, *Icarus*, 106, 210
- Ikoma, M., Nakazawa, K., & Emori, H. 2000, *ApJ*, 537, 1013
- Johansen, A. & Youdin, A. 2007, *ApJ*, 662, 627
- Johnson, J. A., Marcy, G. W., Fischer, D. A., Henry, G. W., Wright, J. T., Isaacson, H., & McCarthy, C. 2006, *ApJ*, 652, 1724
- Kley, W., D'Angelo, G., & Henning, T. 2001, *ApJ*, 547, 457
- Kley, W. & Dirksen, G. 2006, *A&A*, 447, 369
- Kokubo, E. & Ida, S. 1996, *Icarus*, 123, 180
- . 1998, *Icarus*, 131, 171
- Langkowski, D., Teiser, J., & Blum, J. 2008, *ApJ*, 675, 764
- Laughlin, G., Steinacker, A., & Adams, F. C. 2004, *ApJ*, 608, 489
- Li, H., Colgate, S. A., Wendroff, B., & Liska, R. 2001, *ApJ*, 551, 874
- Lin, D. N. C., Bodenheimer, P., & Richardson, D. C. 1996, *Nature*, 380, 606
- Lin, D. N. C. & Papaloizou, J. 1986, *ApJ*, 307, 395
- Lubow, S. H., Seibert, M., & Artymowicz, P. 1999, *ApJ*, 526, 1001
- Luhman, K. L., Adame, L., D'Alessio, P., Calvet, N., McLeod, K. K., Bohac, C. J., Forrest, W. J., Hartmann, L., Sargent, B., & Watson, D. M. 2007, *ApJ*, 666, 1219
- Lynden-Bell, D. & Pringle, J. E. 1974, *MNRAS*, 168, 603
- Masset, F. S. 2001, *ApJ*, 558, 453
- Masset, F. S. & Ogilvie, G. I. 2004, *ApJ*, 615, 1000
- Masset, F. S. & Papaloizou, J. C. B. 2003, *ApJ*, 588, 494
- Matsumura, S. & Pudritz, R. E. 2003, *ApJ*, 598, 645
- . 2006, *MNRAS*, 365, 572
- Matsumura, S., Pudritz, R. E., & Thommes, E. W. 2007, *ApJ*, 660, 1609
- Menou, K. & Goodman, J. 2004, *ApJ*, 606, 520
- Morbidelli, A., Crida, A., Masset, F., & Nelson, R. P. 2008, *A&A*, 478, 929
- Murray, N., Hansen, B., Holman, M., & Tremaine, S. 1998, *Science*, 279, 69
- Muzerolle, J., Calvet, N., Briceño, C., Hartmann, L., & Hillenbrand, L. 2000, *ApJL*, 535, L47
- Nelson, R. P. & Papaloizou, J. C. B. 2004, *MNRAS*, 350, 849
- Paardekooper, S.-J. & Mellema, G. 2008, *A&A*, 478, 245
- Papaloizou, J. C. B. 2002, *A&A*, 388, 615
- Papaloizou, J. C. B. & Larwood, J. D. 2000, *MNRAS*, 315, 823
- Pollack, J. B., Hubickyj, O., Bodenheimer, P., Lissauer, J. J., Podolak, M., & Greenzweig, Y. 1996, *Icarus*, 124, 62
- Rafikov, R. R. 2004, *AJ*, 128, 1348
- Robberto, M., Beckwith, S. V. W., & Panagia, N. 2002, *ApJ*, 578, 897
- Sano, T., Miyama, S. M., Umebayashi, T., & Nakano, T. 2000, *ApJ*, 543, 486
- Sekiya, M. 1998, *Icarus*, 133, 298
- Semenov, D., Wiebe, D., & Henning, T. 2004, *A&A*, 417, 93
- Shakura, N. I. & Sunyaev, R. A. 1973, *A&A*, 24, 337
- Shu, F. H., Johnstone, D., & Hollenbach, D. 1993, *Icarus*, 106, 92
- Sicilia-Aguilar, A., Hartmann, L. W., Fűrész, G., Henning, T., Dullemond, C., & Brandner, W. 2006, *AJ*, 132, 2135
- Tanaka, H., Takeuchi, T., & Ward, W. R. 2002, *ApJ*, 565, 1257
- Tanigawa, T. & Watanabe, S.-i. 2002, *ApJ*, 580, 506
- Thommes, E. W. 2005, *ApJ*, 626, 1033
- Thommes, E. W., Duncan, M. J., & Levison, H. F. 2003, *Icarus*, 161, 431
- Thommes, E. W., Matsumura, S., & Rasio, F. A. 2008, *Science*, 321, 814
- Udry, S. & Santos, N. C. 2007, *ARA&A*, 45, 397
- Ward, W. R. 1997, *Icarus*, 126, 261
- Weidenschilling, S. J. 1977, *MNRAS*, 180, 57
- . 1995, *Icarus*, 116, 433
- Wisdom, J. & Holman, M. 1991, *AJ*, 102, 1528
- Youdin, A. & Johansen, A. 2007, *ApJ*, 662, 613
- Youdin, A. N. & Shu, F. H. 2002, *ApJ*, 580, 494

We thank the anonymous referee for useful comments. Our simulations were carried out on computer clusters of the SHARCNET HPC Consortium at McMaster University. S. M. is supported by McMaster University, and Northwestern University. R. E. P. is supported by a grant from the National Science and Engineering Research Council of Canada (NSERC). E. W. T. is supported by a grant from NSERC, and during earlier parts of this work, by the Spitzer Space Telescope Theoretical Research Program and Northwestern University.